

DOI: <https://doi.org/10.37434/tpwj2024.01.03>

IMPACT OF HEAT TREATMENT ON MECHANICAL PROPERTIES OF JOINTS DURING ELECTRON BEAM WELDING OF 2219 ALLOY

V.V. Skryabinsky, V.M. Nesterenkov, M.O. Rusynyk

E.O. Paton Electric Welding Institute of the NASU
11 Kazymyr Malevych Str., 03150, Kyiv, Ukraine

ABSTRACT

Plates of 2219 alloy of 40 mm thickness were joined by electron beam welding. The effect of sequence of welding and heat treatment operations on the mechanical properties of the joints and distribution of hardness in the HAZ were studied. It was established that the plates of 2219 alloy that were quenched before welding and artificially aged after welding, have the highest strength. Aging improves the ultimate strength of the joints from 300–315 to 385–395 MPa, and hardness of the weld and HAZ metal increases by 5–10 *HRB*. In the study of the joint microstructure it was found that a region of high-temperature recovery of the hardened state is located at a distance of about 1.0 mm from the fusion line in the HAZ. It is characterized by an increase in hardness after aging to the level of base metal hardness. Measuring the welding thermal cycles it was found that the maximum heating temperature of this region is about 590 °C. Next the annealing region is located. In this region, a decrease in the metal hardness by 2–3 *HRB* is observed. For welding speed of 20 mm/s, the HAZ width is about 8 mm.

KEYWORDS: electron beam welding, aluminium alloy, welded joints, heat treatment, mechanical properties, ultimate strength

INTRODUCTION

2219 alloy of Al–6Cu alloying system is a heat-hardenable alloy, the maximal mechanical properties of which are achieved after quenching and artificial aging. Due to its excellent mechanical properties, corrosion resistance and weldability, it has been used to produce welded structures for more than 50 years now. However, improvement of welded joint quality and stability of their mechanical properties still remain a relevant task [1, 2]. Nonconsumable electrode argon-arc welding is usually used to join thin blanks of 2219 alloy, and over the recent decades friction stir welding has become widely accepted. Electron beam welding is used to join thick parts.

With any fusion welding process, welded joint strength will be lower than that of the base metal. This is related to the presence of a region of remelted metal and HAZ adjacent to it. Postweld heat treatment of the joints is performed to improve the joint strength.

Mechanical properties of 2219 alloy welded joints depend not only on heat treatment temperature and time, namely on the sequence of quenching, artificial aging and welding performance. Maximal mechanical properties of welded joints are achieved by conducting full postweld heat treatment (quenching and aging). Such an effect of strength increase is observed both for welding of quenched and artificially aged [3], and annealed semi-finished products [4]. In those cases, when large-sizes products are welded, and it is im-

possible or difficult to quench them, only artificial aging is performed after welding. In work [5] it is shown that postweld artificial aging improves the structure and mechanical properties of welded joints.

In welding aluminium alloys, there is a certain correlation between metal strength and hardness, which, in their turn, are determined by its structure [6]. Artificial aging after welding helps revealing the nature of structural transformations and state of the solid solution in the HAZ in such alloys. The degree of HAZ metal strengthening at artificial aging allows determination of the regions of high-temperature recovery of the quenched state, degree of annealing and presence of low-temperature recovery [7]. Changes in the metal structure in these regions will be visible in microsections, and measurement of welding thermal cycles allows determination of temperatures, at which these changes occur [8].

OBJECTIVE OF THE WORK

The objective of the work is to determine the sequence of quenching, artificial aging and welding operations, at which maximal mechanical properties of welded joints on large-sized products from 2219 aluminium alloy plates are achieved.

MATERIALS AND INVESTIGATION PROCEDURE

The nature of weld formation, hardness distribution in the welded joint cross-section, macro- and microstructure in the metal of the weld and HAZ, as well

Table 1. Chemical composition of 2219 alloy

Weight fraction of chemical elements, %								
Al	Cu	Mn	Mg	Fe	Si	Zn	Zr	Ti
Base	5.8–6.8	0.2–0.4	0.02	0.3	0.2	0.1	0.1–0.25	0.02–0.1

Table 2. EBW mode parameters

Welding speed, mm/s	Accelerating voltage, kV	Welding current, mA	Focus	Scan pattern	Beam scanning amplitude, mm	Beam scanning frequency, Hz
20	60	440	Sharp	Circle	0.5	630

as mechanical properties of the joints were studied. Investigations were conducted on 2219 alloy plates 40 mm thick. State of delivery is T-351 (quenching + mechanical deformation + natural aging). The alloy chemical composition is given in Table 1.

Welding was conducted in UL-209M unit with power supply from ELA 60/60 source with 60 kV accelerating voltage. Welding mode parameters (Table 2) were selected so as to ensure complete penetration of the butt in one pass with formation of weld reinforcement and reverse bead.

Hardness of the weld and HAZ metal was measured by Rockwell instrument with load on the steel sphere $P = 600$ N. Hardness measurements of the metal of the weld and HAZ were conducted on transverse sections for four variants of the sequence of welding and heat treatment operations: 1 — quenching — artificial aging — welding; 2 — quenching — artificial aging — welding — artificial reaging; 3 — annealing — welding; 4 — annealing — welding — artificial aging.

Electron beam is a linear heat source and, therefore, the temperature across the plate thickness is regarded to be stable. In this case, the thermal cycles in EBW of 40 and 10 mm plates will coincide. In order to simplify the experiments, the thermal cycles were recorded at EBW of 2219 alloy plates of 10 mm thickness. An EBW mode was selected, which at welding speed of 20 mm/s, ensured producing a 2 mm wide weld with parallel fusion boundaries.

Temperature on the plate surface was measured by chromel-alumel thermocouples, made from 0.1 mm wires. Thermocouple junctions were caulked into a recess on the plate surface at 2, 4 and 6 mm distance from the weld axis, which at 2 mm weld width was equal to 1, 3 and 5 mm from the fusion line, respectively. Thermocouple readings were recorded by a high-speed recording voltmeter with 100 mm/s speed of tape pulling.

Welded joint structure was revealed by electrolytical polishing and additional chemical etching in 25 % aqueous solution of fluoric acid. The microstructure was examined in an optical metallographic microscope Neophot-32, fitted with Olympus C-500 digital camera.

Mechanical properties of the samples were studied for three variants of the sequence of welding and heat treatment operations: 1 — quenching — artificial aging — welding; 2 — quenching — artificial aging — welding — artificial reaging; 3 — quenching — welding — artificial aging. Artificial aging was conducted at the temperature of 175 ± 5 °C for 19 h with cooling in air.

Ultimate strength was determined by tensile testing of standard round samples with 4 mm diameter of the working part. Impact bend testing was performed on Charpy samples with a notch in the weld metal. Samples for testing were cut out across the weld, placing the weld in the sample center.

INVESTIGATION RESULTS AND THEIR DISCUSSION

Transverse section of a joint of 2219 alloy plates is shown in Figure 1. During welding, formation of weld reinforcement and reverse bead was guaranteed (Figure 2). EBW process proceeded without liquid metal splashing. Slight spatter was observed from the weld root side.

Welding mode ensured producing narrow welds of approximately 2.0 mm width with parallel fusion boundaries. Such a shape of the weld promotes reduction of residual welding deformations of the structure.


Figure 1. Transverse section of a joint of 2219 alloy plates 40mm thick

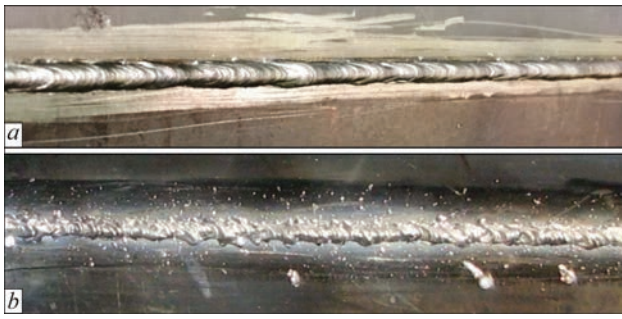


Figure 2. Appearance of the weld of a joint of 2219 alloy plates 40 mm thick from the side of electron beam entrance (a) and exit (b)

Results of welded joint hardness measurements are shown in Figure 3. Base metal hardness in the quenched and aged states is equal to 96 HRB, and weld metal hardness is 73 HRB. One can see that metal hardness at 1.0 mm distance from the fusion line is by 1–2 HRB higher than that of metal hardness at 2.0–3.0 mm distance from the weld. Artificial aging of the joints after welding increases weld metal hardness by 10 HRB, and metal hardness in the HAZ rises by 3–5 HRB. After welding, HAZ width is equal to approximately 8 mm.

When welding annealed plates, weld metal hardness (Figure 4) is on the level of base metal hardness (72–73 HRB), and the HAZ metal located at 1.0 mm distance from the fusion line shows the highest hardness. When moving away from the fusion line, metal hardness becomes lower. Artificial aging of welded joints strengthens the weld and HAZ metal, and their hardness here increases by 5–10 HRB.

Changes in HAZ metal hardness are the consequence of metallurgical processes, proceeding in the metal under the impact of welding thermal cycle. The welding thermal cycles were recorded, in order to determine the temperatures, at which these changes occur. Experimentally obtained characteristic curves of temperature change during heating and cooling under the impact of the welding thermal cycle are shown in Figure 5. Maximal heating temperatures for points located at 2.0, 4.0 and 6.0 mm distance from the weld

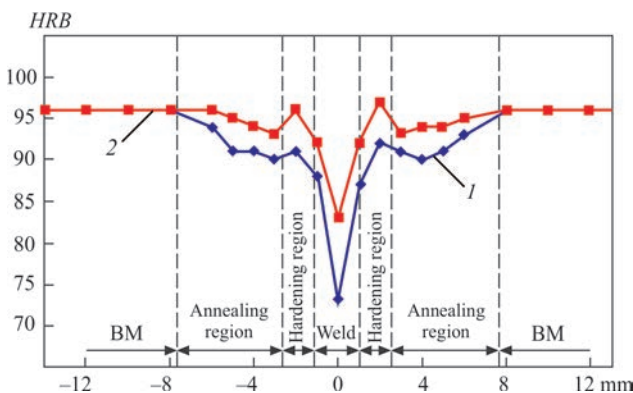


Figure 3. Hardness distribution in the cross-section of joints of quenched and artificially-aged 2219 alloy plates 40 mm thick; 1 — welded joints; 2 — welded joints reaged artificially after welding

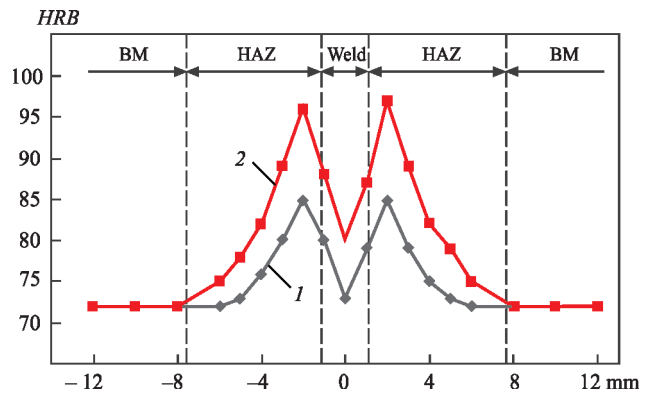


Figure 4. Hardness distribution in the cross-section of joints of annealed 2219 alloy plates 40 mm thick; 1 — welded joints; 2 — welded joints artificially aged after welding

axis (or 1.0, 3.0 and 5.0 mm from the fusion line) were equal to 590, 440 and 300 °C, respectively.

Weld metal microstructure (Figure 6, a) is dispersed; it consists of a matrix — aluminium-based α -solid solution and CuAl_2 (θ -phase), precipitating along the boundaries and chaotically in the grain bulk. CuAl_2 (θ -phase) is the main strengthening phase in alloys of this system. The fusion line (Figure 6, b) is well-formed, and no defects were found on the fusion line. HAZ width is up to 10 mm from the fusion line. Low-melting eutectic interlayers form in the HAZ region adjacent to the fusion line. A region of high-temperature recovery of the quenched state is located at 0.5–3.0 mm distance from the fusion line (Figure 3). It is characterized by a hardness increase after aging to base metal hardness level. The annealing region is next. A lowering of metal hardness by 2–3 HRB is observed in this region.

The influence of the sequence of welding and heat treatment operations on the mechanical properties of 2219 alloy welded joints was studied. Quenched plates and plates after full heat treatment (quenching and artificial aging) were welded. Quenched plates and part of the plates after full heat treatment were subjected to postweld artificial aging.

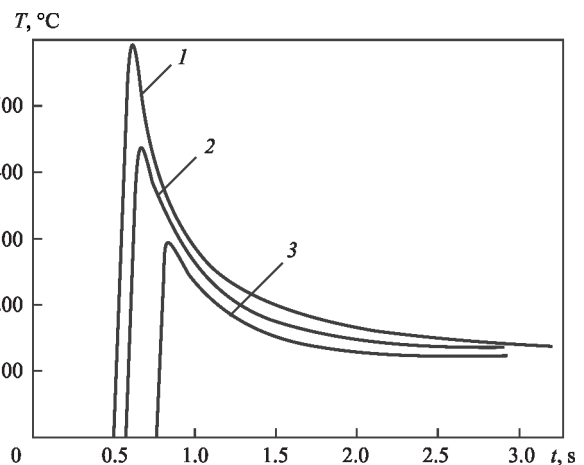


Figure 5. Thermal cycles of points on the surface of 2219 alloy plate at EBW with 20 mm/s speed (L — distance from weld middle; 1 — 2 mm; 2 — 4; 3 — 6)

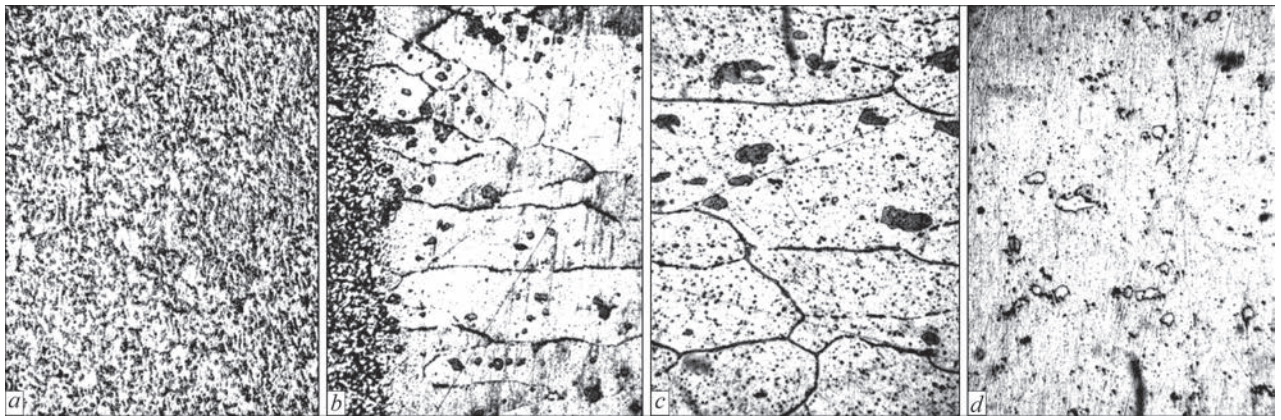


Figure 6. Microstructure of weld (*a*) and HAZ (*b–d*) metal at EBW of 2219 alloy plates (*a* — weld metal; *b* — fusion line; *c* — high-temperature recovery region; *d* — annealing region), ($\times 500$, reduced 2 times)

Table 3. Mechanical properties of joints of 2219 alloy plates 40 mm thick in different initial states of base metal and at further heat treatment

Kind of treatment		Ultimate strength, σ_{ult} , MPa	Relative elongation, δ , %	Impact toughness, KCV, kgf·m/cm ²
Before welding	After welding			
Quenching and artificial aging	Without heat treatment	<u>300.0–315.0</u> 308.7	<u>3.0–4.0</u> 3.3	<u>4.2–4.7</u> 4.5
	Artificial aging	<u>357.0–367.5</u> 361.7	<u>2.6–5.7</u> 3.6	<u>1.4–1.7</u> 1.5
Quenching	Artificial aging	<u>385.0–395.0</u> 388.7	<u>3.0–3.0</u> 3.0	<u>2.9–3.2</u> 3.0

Note. The numerator gives the minimal and maximal values from 3 measurements; the denominator gives the average values.

Results of welded joint testing for static tension and impact bending are shown in Table 3.

Electron beam welding is characterized by high rates of heating and cooling of the metal of the weld and HAZ. Such cooling rates in EBW of 2219 alloy will promote formation of copper solid solution in the weld metal. At further artificial aging precipitation of strengthening phases and increase of weld metal hardness occur, respectively.

Hardness increase at 1 mm distance from the fusion line is due to short-time heating of the metal to quenching temperature and rapid cooling. Maximal temperature of metal heating is about 590 °C. This zone is usually called the zone of high-temperature recovery of the quenched state. After conducting artificial aging, metal hardness is increased here up to the level of base metal hardness in the state after quenching and artificial aging. This zone was earlier revealed only in arc-welded joints [7, 8].

Annealing zone, called the low-temperature recovery zone, is located farther from the fusion line. At the beginning of this zone the maximal temperature was 440 °C, and in the middle part it was approximately 300 °C. Hardness of the metal of the weld and high-temperature recovery zone at EBW of heat-treated and annealed plates is the same and independent of

the metal initial condition. As one can see from Figures 3 and 4, in welding heat-hardened plates of 2219 alloy the HAZ metal is softened, and in welding of annealed plates, on the contrary, the metal strength in the HAZ becomes higher.

In case of welding plates which have passed the full heat treatment cycle, the ultimate strength of the joints was equal to 300.0–315.0 MPa. It was possible to increase the ultimate strength to the level of 357.0–367.5 MPa, having conducted artificial aging. Here, the impact toughness decreased from 4.2–4.7 to 1.4–1.7 kgf·m/cm². Postweld artificial aging operation is more favourable, compared to aging before welding. In this case, the ultimate strength of the joints rises to 385–395 MPa, and impact toughness decreases only slightly to the level of 2.9–3.2 kgf·m/cm². Relative elongation changes only slightly here.

CONCLUSIONS

1. At EBW of quenched plates from 2219 alloy the maximal mechanical properties of welded joints are achieved by conducting postweld artificial aging.

2. Artificial aging of welded joints of 2219 alloy plates increases the hardness of weld and HAZ metal by 5–10 HRB.

3. When measuring HAZ hardness of 2219 alloy joints produced by EBW, a region of high-temperature

recovery of the quenched state with hardness increase was found at approximately 1 mm distance from the fusion line. After artificial aging the hardness of this region is increased to the level of base metal hardness in the heat-hardened state.

REFERENCES

1. Zhang, D.K., Wang, G.Q., Wu, A.P. et al. (2019) Study on the inconsistency in mechanical properties of 2219 aluminium alloy TIG-welded joints. *J. of Alloys and Compounds*, 777(10), 1044-1053. <https://www.sciencedirect.com/science/article/abs/pii/S0925838818338568>
2. Tianyi Zhao, Yue Zhao, Zhandong Wan et al. (2023) "Anneal" softening effect of 2219-T8 aluminum alloy joint during welding and its influence on prediction of welding residual stresses. *J. Mater. Research Technology*, 24, 5202–5214. <https://www.sciencedirect.com/science/article/pii/S2238785423007871>
3. Zhang, D.K., Wang, G.Q., Wu, A.P. et al. (2019) Effects of post-weld heat treatment on microstructure, mechanical properties and the role of weld reinforcement in 2219 aluminium alloy TIG-welded joints. <https://www.amse.org.cn/article/2019/1006-7191/1006-7191-32-6-684.shtml>
4. Chen, Y. C., Liu, H. J., Feng, J. C. (2005) Effect of post-weld heat treatment on the mechanical properties of 2219-O friction stir welded joints. *J. Mater. Sci.*, 41(1), 297–299. <https://www.researchgate.net/publication/227050248>
5. Malarvizhi, S., Raghukandan, K., Viswanathan, N. (2008) Effect of post weld aging treatment on tensile properties of electron beam welded AA2219 aluminum alloy. *Int. J. Adv. Manuf. Technol.*, 37, 294–301. <https://link.springer.com/article/10.1007/s00170-007-0970-7>
6. Rabkin, D.M., Lozovskaya, A.V., Sklabinskaya, I.E. (1992) *Metals science of aluminium and its alloys*. Kyiv, Naukova Dumka [in Russian].
7. Lozovskaya, A. V., Chaika, A. A., Bondarev, A. A. et al. (2001) Softening of high-strength aluminium alloys in different methods of fusion welding processes. *The Paton Welding J.*, 3, 13–17. <https://patonpublishinghouse.com/as/pdf/2001/as200103all.pdf>
8. Lan-Qiang Niu, Xiao-Yan Li, Liang Zhang, Xiao-Bo Liang, Mian Li (2017) Correlation between microstructure and mechanical properties of 2219-T8 aluminum alloy Joints by VP-TIG welding. *J. Acta Metallurgica Sinica*, 30(5), 438–446. DOI: <https://doi.org/10.1007/s40195-016-0516-9>

ORCID

V.V. Skryabinsky: 0000-0003-4470-3421,
V.M. Nesterenkov: 0000-0002-7973-1986,
M.O. Rusnyk: 0000-0002-7591-7169

CONFLICT OF INTEREST

The Authors declare no conflict of interest

CORRESPONDING AUTHOR

V.V. Skryabinsky
E.O. Paton Electric Welding Institute of the NASU
11 Kazymyr Malevych Str., 03150, Kyiv, Ukraine.
E-mail: skriabinski.vv.555@gmail.com

SUGGESTED CITATION

V.V. Skryabinsky, V.M. Nesterenkov, M.O. Rusnyk (2024) Impact of heat treatment on mechanical properties of joints during electron beam welding of 2219 alloy. *The Paton Welding J.*, 1, 22–26.

JOURNAL HOME PAGE

<https://patonpublishinghouse.com/eng/journals/tpwj>

Received: 12.10.2023

Received in revised form: 15.12.2023

Accepted: 17.01.2024



**VII INTERNATIONAL
CONFERENCE ON WELDING
AND RELATED TECHNOLOGIES**

7-10 October 2024 Kyiv, Ukraine

www.wrt2024.com.ua